Molecular Immunology 114 (2019) 62–71

Contents lists available at ScienceDirect

Molecular Immunology

journal homepage: www.elsevier.com/locate/molimm

Optimal combination of beneficial mutations for improved ADCC effector function of aglycosylated antibodies

Hyun Woung Yoon[a,1], Migyeong Jo[a,b,1], Sanghwan Ko[a,b], Hyeong Sun Kwon[c], Chung Su Lim[d], Byoung Joon Ko[d], Ji Chul Lee[c], Sang Taek Jung[b,*]

[a] Department of Applied Chemistry, Kookmin University, Seongbuk-gu, Seoul 02707, Republic of Korea
[b] Department of Biomedical Sciences, Graduate School of Medicine, Korea University, Seongbuk-gu, Seoul 02841, Republic of Korea
[c] SG Medical, 3-11, Ogeum-ro 13-gil, Songpa-gu, Seoul, 05548, Republic of Korea
[d] New Drug Development Center, Osong Medical Innovation Foundation, 123, Cheongju, Chungcheongbuk-do 28160, Republic of Korea

ARTICLE INFO

Keywords:
Aglycosylated IgG
Effector functions
Fc engineering
FcγRIIIa
Antibody-dependent cell-mediated cytotoxicity

ABSTRACT

The Fc region of IgG antibodies is crucial for binding to Fc receptors expressed on the surfaces of various immune leukocytes and eliciting therapeutic effector functions such as clearance of antibody-opsonized tumor cells. Despite abrogated Fc gamma receptor (FcγR) binding and therapeutic effector function in the absence of *N*-linked glycosylation at Asn297, the aglycosylated Fc region of IgG antibodies has bioprocessing advantages such as the absence of glycan heterogeneity and simple bacterial antibody production. Therefore, these antibodies have been comprehensively engineered as effector functional units for human therapy. In this work, we constructed a huge library of Fc variants with combinations of 25 beneficial mutations that were previously identified to improve binding of glycosylated or aglycosylated Fc regions to human FcγRs in previous studies. High-throughput screening of the resulting library led to the identification of an aglycosylated Fc variant that exhibited almost double the antibody-dependent cell-mediated cytotoxicity than wild-type glycosylated Fc. All mutations in this aglycosylated Fc variant were derived from previously identified beneficial mutations for engineered aglycosylated Fc variants as opposed to glycosylated variants, suggesting that significantly different sets of beneficial mutations are necessary to improve the effector function of aglycosylated Fc.

1. Introduction

The significance of monoclonal antibodies in human therapy is increasing rapidly (Reichert, 2017), as is the repertoire of commercially available monoclonal antibody therapeutics. The monoclonal antibody drug market is projected to be worth over 130 billion USD in 2022 (Grilo and Mantalaris, 2019; Walsh, 2018). The reasons for the clinical success of therapeutic antibodies is their exceptionally high target specificity, low toxicity, and antibody Fc-mediated effector functions, which cannot be obtained using conventional small-molecule chemical drugs.

IgG antibodies bound to target antigens on tumor cells recruit a variety of immune leukocytes via interactions between the Fc region of IgG and Fc gamma receptors (FcγRs) expressed on the surfaces of immune effector cells. Immune cells activated in this way release cytotoxic granules and induce phagocytic mechanisms to clear tumor cells, which are called antibody-dependent cell-mediated cytotoxicity (ADCC) and antibody-dependent cell-mediated phagocytosis (ADCP), respectively (Park et al., 2016). To improve the efficacy of therapeutic antibodies compared to antibodies containing the wild-type Fc backbone, various Fc engineering strategies have been employed, and many global biopharmaceutical companies and institutions are conducting research to isolate Fc variants with enhanced therapeutic effector functions.

Based on *in silico* screening followed by analyses of the interaction between FcγRs and IgG Fc variant candidates, Xencor generated glycosylated Fc variants with enhanced FcγRIIIa binding. Alemtuzumab and trastuzumab with specific mutations (S239D/I332E or S239D/I332E/A330L) exhibited greater than 100-fold higher FcγRIIIa binding affinity and significantly better ADCC effector function than counterpart IgG containing wild-type Fc (Lazar et al., 2006). The same

Abbreviations: ADCC, antibody-dependent cell-mediated cytotoxicity; Fc, fragment crystallizable; FcγR, Fc gamma receptor; FcRn, neonatal Fc receptor; GlycoT, glycosylated trastuzumab; HEK293F, human embryonic kidney 293F; MHC, major histocompatibility complex; PBMC, peripheral blood mononuclear cells

* Corresponding author.
E-mail address: sjung@korea.ac.kr (S.T. Jung).
[1] These authors equally contributed to the work.

https://doi.org/10.1016/j.molimm.2019.07.007
Received 8 March 2019; Received in revised form 10 July 2019; Accepted 10 July 2019
Available online 20 July 2019

company identified the G236A mutation, which enhanced ADCP effector function through increased binding specificity for FcγRIIa (activating) over FcγRIIb (inhibitory) (Richards et al., 2008). In subsequent work, an Fc variant with two mutations (S267E/L328F) that displayed better than 400-fold improved binding for FcγRIIb was isolated, and an anti-CD19 antibody with these double mutations could effectively suppress B cell receptor activation (Chu et al., 2008). Macrogenics screened an Fc variant library using yeast surface display and isolated an Fc variant (L235V/F243L/R292P/Y300L/P396L) with significantly greater binding affinity for FcγRIIIa than FcγRIIb, enabling improved clearance of cancer cells expressing low levels of tumor-specific antigens on their surfaces (Nordstrom et al., 2011; Stavenhagen et al., 2007).

The homodimeric human IgG Fc region contains a pair of *N*-linked glycans appended to Asn297 in each Fc polypeptide. The presence of oligosaccharides has a strong effect on the structural flexibility of the upper CH2 region of Fc (Ju et al., 2015), and the removal of the *N*-linked glycans abrogates all human FcγR binding and subsequent effector functions such as ADCC and ADCP (Park et al., 2016). Therefore, Fc engineering studies to date have mostly focused on antibodies with a glycosylated Fc region in which *N*-linked glycans are attached to Asn297. However, comprehensive directed evolution of aglycosylated Fc regions using a high-throughput library screening facilitated the isolation of aglycosylated IgG Fc variants with comparable or improved FcγR binding compared to that of glycosylated IgG Fc variants. Using a yeast surface display system, Sazinsky et al. screened an Fc variant library with randomized amino acids at the C′E loop of the Fc region and isolated an aglycosylated Fc variant (S298G/T299A) that exhibited comparable FcγRIIa binding and *in vivo* effector function as glycosylated wild-type Fc (Sazinsky et al., 2008). The same strategy was used to isolate an FcγRIIIa-binding aglycosylated Fc variant (T299A/K326I/A327Y/L328G) (Wittrup et al., 2014).

Bacterial display of homodimeric aglycosylated Fc permitted the identification of critical mutations for improved FcγR binding affinity and specificity. Two mutations in the CH3 region (E382V/M428I) stabilized the conformation of the lower hinge and upper CH2 regions of Fc for better binding to FcγRI, which elicited dendritic cell-mediated tumor cell killing (Ju et al., 2015; Jung et al., 2010). Via further engineering of the aglycosylated Fc variant, additional mutations (Q295R/L328W/P331A/I332Y/E382V/M428L) that increased FcγRI binding were identified (Jung et al., 2014). In addition, display of aglycosylated full-length IgG and high-throughput library screening allowed the generation of an aglycosylated Fc variant (S298G/T299A/E382V/N390D/M428L) that exhibited selective binding to activating FcγRIIa over inhibitory FcγRIIb and significantly enhanced ADCP effector function. Recently, we identified mutations (V264E/S298G/T299A/K326I/A327Y/L328G/T350A/E382V/N390D/M428L) in aglycosylated Fc that conferred higher FcγRIIIa binding than that of wild-type glycosylated IgG (Jo et al., 2018b).

In this study, we constructed an aglycosylated Fc shuffled library comprising combinations of beneficial mutations discovered through engineering of either glycosylated or aglycosylated IgG Fc variants. Using high-throughput library screening, we identified the best combination of previously identified mutations for enhanced binding of aglycosylated Fc to FcγRIIIa. In addition, we examined whether mutations conferring improved FcγR binding affinity for glycosylated Fc enhanced the binding affinity of aglycosylated Fc for FcγRIIIa.

2. Materials and methods

2.1. Chemicals and reagents

All oligonucleotides and plasmids used in this study are listed in Table 1 and Supplementary Table S1, respectively. Ligase and all restriction enzymes were purchased from New England Biolabs (Ipswich, MA). Terrific broth (TB), yeast extract, and nutrient broth were obtained from BD Biosciences (Bergen, NJ). Agar was obtained from Affymetrix (Santa Clara, OH). Isopropyl-1-thio-β-*D*-galactopyranoside (IPTG), glycerol, and EDTA were acquired from Biosesang (Seongnam, South Korea). TMB, anti-C1q antibody, and an Alexa 488 labeling kit were purchased from Thermo Fisher Scientific (Waltham, MA). Anti-streptavidin antibody was obtained from GeneTex (Irvine, CA). High binding 96-well plates were purchased from Corning (Corning, NY). FcγRI, goat anti-GST-HRP conjugate, and the Rapi-Fluor labeling kit were obtained from R&D Systems (Minneapolis, MN), GE Healthcare (Piscataway, NJ), and Waters (Milford, MA), respectively. Mouse anti-His-HRP conjugate, C1q, and all other chemicals were purchased from Sigma Aldrich (Saint Louis, MO) unless stated otherwise. Dip and Read™ Amine Reactive Second-Generation (AR2G) biosensors and all reagents for analyses using these biosensors were purchased from Pall Fortebio (Menlo Park, CA).

2.2. Preparation of Fc receptors

Monomeric FcγRIIIa-158V gene was PCR-amplified using pMAZ-FcγRIIIa-158V-GST as a template (Jo et al., 2018b) and primers (HW#39 and HW#40), digested using *Bss*HII and *Xba*I, and ligated into pMAZ vector digested using the same restriction enzymes to generate pMAZ-FcγRIIIa-158V-His. Plasmids encoding dimeric Fc receptors (FcγRIIa-131H-GST, FcγRIIa-131R-GST, FcγRIIb-GST, FcγIIIa-158V-GST, FcγRIIIa-158F-GST, and FcRn-GST) and tetrameric FcγRIIIa-158V-Streptavidin-His were prepared as described previously (Jo et al., 2018b). The resulting plasmids (pMAZ-FcγRIIa-131H-GST, pMAZ-FcγRIIa-131R-GST, pMAZ-FcγRIIb-GST, pMAZ-FcγRIIIa-158V-GST, pMAZ-FcγRIIIa-158F-GST, and pMAZ-FcRn-GST) were transfected into HEK293F cells by polyethylenimine (PEI) transfection followed by incubation for 7 days in 300 mL of GIBCO FreeStyle™ medium (Thermo Fisher Scientific, Carlsbad, CA) at 37°C. After centrifugation at 6000 × *g* for 15 min, culture supernatants were mixed with 12 mL of 25 × PBS and filtered through a 0.22-μm bottle top filter (Thermo Fisher Scientific, Waltham, MA). Filtered supernatants from cells expressing GST-fused dimeric Fc receptors (FcγRIIa-131H-GST, FcγRIIa-131R-GST, FcγRIIb-GST, FcγIIIa-158V-GST, FcγRIIIa-158F-GST, and FcRn-GST) were purified as reported previously (Jo et al., 2018b). Monomeric and tetrameric FcγRIIIa-158 V proteins were purified using nickel-NTA resin (Qiagen, Hilden, Germany) equilibrated in 1 × PBS (pH 7.4). After binding of supernatants to the resin at 4°C overnight and washing with 20 mL of 10 mM imidazole buffer and 20 mL of 20 mM imidazole buffer, monomeric FcγRIIIa-158V-His and tetrameric FcγRIIIa-158V-streptavidin-His were eluted with 4 mL of 250 mM imidazole buffer. Then, the buffer of the purified FcγRs was exchanged with 1 × PBS via ultrafiltration through a 3-kDa MW cutoff membrane (MilliporeSigma, Burlington, MA). One milligram of purified tetrameric FcγRIIIa-158 V was fluorescently labeled using an Alexa 488 labeling kit according to the manufacturer's guidelines.

2.3. Library construction

Overlapping PCR was conducted using three sets of primers (HW#1–6, HW#7–15, and HW#16–20). After PCR assembly of the resulting three fragments using the primer sets HW#21/HW#23, HW#24/HW#25, and HW#26/HW#22, PCR products were digested using *Sfi*I restriction endonuclease, ligated into the pBLA plasmid (Ju et al., 2017) for C-terminal β-lactamase fusion, and transformed in *Escherichia coli* Jude-1 strain (F′ [Tn*10*(Tet^r) proAB$^+$ *lacI*^{q} Δ(*lacZ*)M15] *mcrA* Δ(*mrr-hsdRMS-mcrBC*) 80d*lacZ*ΔM15 Δ*lacX74 deoR recA1 araD139* Δ(*ara leu*)7697 *galU galK rpsL endA1 nupG*) (Kawarasaki et al., 2003). After plating on an LB agar plate supplemented with 40 μg/mL chloramphenicol and 20 μg/mL ampicillin and incubation at 37°C overnight, plasmids encoding the three in-frame selected fragments were PCR-amplified using primers sets HW#21/HW#27, HW#28/HW#29, and HW#30/HW#22, and full-length Fc variant genes were

Table 1
Plasmids used in the current study.

Plasmid	Relevant characteristics	Reference or source
pAK200	Cm^r, *Lac* promoter, *gpIII* gene in	Krebber et al. (1997)
pBLA	Cm^r, *Lac* promoter, *BLA* gene in after *VHH* gene	Ju et al. (2017)
pMAZ-FcγRIIIa-158V-FLAG-Streptavidin-His	*FcγRIIIa-158V-FLAG-Streptavidin-6× His* gene in pMAZ-IgH-GlycoT	Jo et al. (2018b)
pMAZ-FcγRIIa-131H-GST	*FcγRIIa-131H-GST* gene in pMAZ-IgH-GlycoT	Jo et al. (2018b)
pMAZ-FcγRIIa-131R-GST	*FcγRIIa-131R-GST* gene in pMAZ-IgH-GlycoT	Jo et al. (2018b)
pMAZ-FcγRIIb-GST	*FcγRIIb-GST* gene in pMAZ-IgH-GlycoT	Jo et al. (2018b)
pMAZ-FcγRIIIa-158V-GST	*FcγRIIIa-158V-GST* gene in pMAZ-IgH-GlycoT	Jo et al. (2018b)
pMAZ-FcγRIIIa-158F-GST	*FcγRIIIa-158F-GST gene* in pMAZ-IgH-GlycoT	Jo et al. (2018b)
pMAZ-FcRn-GST	*FcRn-GST* gene in pMAZ-IgH-GlycoT	Jo et al. (2018b)
pMAZ-FcγRIIIa-158V-His	*Monomeric FcγRIIIa-158V* gene with 6× His tag in pMAZ-IgL-GlycoT	Current study
pAK200-Fc-MG48-gpIII	*Fc-MG48* gene in pAK200	Jo et al. (2018b)
pAK200-Fc-HW86-gpIII	*Fc-HW86* gene in pAK200	Current study
pSTJ4-AglycoT	*Trastuzumab* gene in pMAZ360-M18.1-Hum-IgG1	Jung et al. (2010)
pHW1-AglycoT	Inducing MUTR sequence TTGAACTTTAAGAAGGAGATATACAT into pSTJ4-AglycoT	Current study
pHW1-AglycoT-HW86	*Trastuzumab Fc-HW86 mutant H chain* gene in pHW1-AglycoT	Current study
pBAD33-DsbC-Chaperon	Cm^r, *araBAD* promoter	Lee et al. (2014)
pMAZ-IgH-GlycoT	*Trastuzumab H chain* gene in pMAZ-IgH-H23	Jung et al. (2010)
pMAZ-IgL-GlycoT	*Trastuzumab L chain* gene in pMAZ-IgL-H23	Jung et al. (2010)
pMAZ-IgH-AglycoT-HW86	*Trastuzumab Fc-HW86 mutant H chain* gene in pMAZ-IgH- GlycoT	Current study
pAK200-wild-type-Fc-gpIII	*Wild-type Fc* gene in pAK200	Jo et al. (2018b)
pAK200-Fc-T394A-gpIII	*Fc-T394A mutant* gene in pAK200	Current study
pAK200-Fc1004/IYG-gpIII	*Fc1004/IYG mutant* gene in pAK200	Jo et al. (2018b)
pAK200-Fc1004/IYG-T394A-gpIII	*Fc1004/IYG-T394A mutant* gene in pAK200	Current study

recovered via assembly PCR of the three in-frame selected fragments using primers HW#21 and HW#22. After ligation into pBLA using *Sfi*I restriction sites and transformation in Jude-1, plasmids encoding in-frame full-length Fc variants were recovered from transformants on LB agar plates. Following *Sfi*I digestion of the plasmids and ligation into pAK200 (Krebber et al., 1997) using the same restriction enzyme sites, plasmids were transformed into *E. coli* Jude-1 to generate an in-frame selected Fc variant library.

2.4. Library screening and construction of plasmids for the T394A point mutation

E. coli Jude-1 cells harboring plasmids encoding Fc variants were inoculated into 25 mL of TB medium containing 2% glucose and 40 μg/mL of chloramphenicol. After incubation at 37°C for 4 h with shaking at 250 rpm, the culture broth was diluted 1:100 in 100 mL of TB medium and cultivated at 37°C with shaking at 250 rpm until the OD_{600} reached 0.5. Then, the culture broth was cooled to 25°C for 20 min, and 1 mM IPTG was added to induce protein expression. After 5 h of incubation at 25°C with shaking at 250 rpm, cells (8 mL/OD_{600}) were harvested via centrifugation at 14,000 rpm for 1 min, and the pellet was resuspended in 1 mL of Tris-HCl (pH 8.0) for washing. After repeating the washing step, harvested cells were resuspended in 1 mL of STE (0.5 M sucrose, 10 mM Tris-HCl, 10 mM EDTA, pH 8.0) and incubated at 37°C for 30 min with rotating mixing. After centrifugation at 14,000 rpm, resuspension in 1 mL of Solution A (0.5 M sucrose, 20 mM $MgCl_2$, 10 mM MOPS, pH 6.8), and pelleting via centrifugation, cells were resuspended in 1 mL of Solution A supplemented with 20 μL of lysozyme (50 mg/mL) and incubated at 37°C for 15 min with rotating mixing. Following pelleting via centrifugation and resuspension in 1 mL of PBS, a 300 μL aliquot of the resuspended cells was mixed with 700 μL of 1 × PBS containing 20 (for first and second rounds), 5 (third and fourth rounds), or 2.5 nM (fifth round) Alexa 488-conjugated tetrameric FcγRIIIa-streptavidin (Jo et al., 2018b). After 1 h of incubation, fluorescently labeled spheroplasts were harvested, washed in 1 mL of PBS, and diluted in 15 mL of PBS. After filtering through a 40-μm cell strainer (BD Biosciences), spheroplasts with fluorescence signals within the range of the selected gate (3%) were sorted using S3 flow cytometry (Bio-Rad, Hercules, CA). Fc variant genes from sorted spheroplasts were rescued via PCR amplification, ligated into pAK200-Fc-MG48-gpIII (Jo et al., 2018b) using *Sfi*I restriction enzyme sites, and transformed in Jude-1 cells for the next round of sorting. To introduce the T394A point mutation into pAK200-wild-type-Fc-gpIII and pAK200-Fc1004/IYG-gpIII, plasmids amplified by PCR using two primers (HW#37 and HW#38) were treated with *Dpn*I enzyme for 1 h and transformed in *E. coli* Jude-I cells. The resulting Fc variants were verified via standard Sanger sequencing. MFI (Mean fluorescence intensity) values, which can be slightly variable across experiments depending on experimental conditions such as cultivation, spheroplasting, and/or probe labeling, were analyzed using Guava EasyCyte™ (Millipore, Burlington, MA), and the MFI of aglycosylated Fc was used as a reference for each FACS analysis experiment.

2.5. Expression of aglycosylated trastuzumab in E. coli

The untranslated region (5′-GAAGGAGATATACAT-3′) of pSTJ4-AlycoT (Jung et al., 2010), a bicistronic plasmid encoding both the light and heavy chains of trastuzumab IgG, was modified (5′-TTGAACTTTA AGAAGGAGATATACAT-3′) as described previously (Lee et al., 2014) to generate pHW1-AglycoT. pHW1 and a plasmid for chaperone expression (pBAD33-DsbC-Chaperon) (Lee et al., 2014) were co-transformed in *E. coli* MG1655 (F^- λ^- *ilvG*$^-$ *rfb-50 rph-1*). A single transformant colony was inoculated into 5 mL of TB supplemented with 2% glucose, 40 μg/mL of chloramphenicol, and 50 μg/mL of ampicillin. After overnight incubation at 37°C with shaking at 250 rpm, the culture broth was diluted 1:10 in R/2-CM-AMP medium [R/2 medium (Jung et al., 2010) supplemented with 40 μg/mL chloramphenicol and 50 μg/mL ampicillin] for cultivation at 37°C for 16 h. After 20-fold dilution in R/2-CM-AMP medium and incubation at 37°C for 16 h with shaking at 250 rpm, cells were inoculated 1:50 into R/2-CM-AMP medium, and cultivations were repeated for adaptation to the same conditions. Culture broth (200 mL) containing adapted cells was inoculated into a fermenter containing 2 L of R/2-CM-AMP medium and the inoculated medium was incubated at 37°C with 200 rpm agitation. The dissolved oxygen level was controlled to be 40% by adjusting the agitation speed until it reached 1000 rpm, and the flow rate of air/pure oxygen and pH of the medium were maintained by adding a feeding solution (500 g/L glucose, 10 g/L $MgSO_4{\cdot}7H_2O$, and 100 g/L yeast extract) or 50% ammonia solution in a dropwise manner. When the absorbance of the culture broth at 600 nm reached approximately 70, the culture temperature was decreased to 25°C, and after 20 min, the expression of full-length aglycosylated trastuzumab IgG (AglycoT) was induced by adding 1 mM

IPTG and 0.2% (w/v) arabinose. Six hours after induction, cells were harvested via centrifugation at 6000 × *g* for 10 min.

2.6. Purification of aglycosylated trastuzumab from E. coli

Harvested cells were resuspended in 1.2 L of resuspension buffer (100 mM Tris, 10 mM EDTA, 4 mg of lysozyme/g dry cell weight, one tablet of protease inhibitor cocktail (complete, EDTA-free; Roche Diagnostics, Indianapolis, IN), and 1 mM PMSF, pH 7.4) and incubated at 30°C for 16 h with shaking at 250 rpm to release the AglycoT expressed in the *E. coli* periplasm. After centrifugation at 14,000 × *g* for 30 min to remove cell debris, PEI (MP Biomedical, Solon, OH) was added dropwise to the supernatant to a final concentration of 0.2% (w/v), and insoluble aggregates and cell debris were cleared via repeat centrifugation at 14,000 × *g* for 30 min and filtration through a 0.2-μm filter. After mixing the recovered supernatant with Protein A agarose resin (Amicogen, Jinju, Korea) pre-equilibrated in 20 mM sodium phosphate buffer (pH 7.0) and incubation at 4°C for 16 h, the resin was washed with 200 mL of 20 mM sodium phosphate buffer (pH 7.0) and 200 mL of 40 mM sodium citrate buffer (pH 5.0) sequentially, and AglycoT expressed in *E. coli* was eluted by adding 3 mL of 0.1 M glycine (pH 3.0). The eluent was neutralized immediately by adding 40 μL of 1 M Tris solution (pH 9.0) and concentrated using an ultrafiltration unit (3-kDa MW cutoff membrane). The retentate was further purified using a Superdex 200 gel filtration column developed with 1 × PBS (pH 7.4).

2.7. Expression and purification of trastuzumab Fc variants in HEK293F cells

An Fc variant (Fc-HW86) that was PCR-amplified using pAK200-Fc-HW86-gpIII as a template and primers HW#33 and HW#34 was overlapped with trastuzumab VH-CH1 region genes prepared via PCR amplification using pMAZ-GlycoT as a template (Jung et al., 2010) and primers HW#35 and HW#36. Next, trastuzumab Fc variant heavy chain genes were PCR-amplified using primers HW35 and HW#34, digested with the restriction enzymes *Bss*HII and *Xba*I, and ligated into pMAZ-IgH-GlycoT (Jung et al., 2010) to generate a plasmid (pMAZ-IgH-AglycoT-HW86) expressing the trastuzumab Fc variant heavy chain. To express trastuzumab Fc variants (glycosylated trastuzumab: GlycoT; aglycosylated trastuzumab Fc mutant-HW86: AglycoT-HW86; aglycosylated trastuzumab Fc mutant-MG48: AglycoT-MG48) in mammalian cells, pMAZ-IgL-GlycoT (Jung et al., 2010) was co-transfected with either pMAZ-IgH-GlycoT, pMAZ-IgH-AglycoT-HW86, or pMAZ-IgH-AglycoT-MG48 into HEK293 F cells using PEI. Seven days after incubating cells in 300 mL of GIBCO FreeStyle™ medium at 37°C, supernatants were recovered from culture broth via centrifugation at 6000 × *g* for 15 min, mixed with 12 mL of 25 × PBS, and filtered through a 0.22-μm bottle top filter. After binding of the filtrate to 1 mL of Protein A resin equilibrated in 1 × PBS overnight at 4°C and washing of the resin with 50 mL 1 × PBS, GlycoT, AglycoT-HW86, and AglycoT-MG48 were eluted in 3 mL of 0.1 M glycine (pH 3.0), and 120 μL of 1 M Tris (pH 9.0) was immediately added for neutralization. The purified solution was concentrated via ultrafiltration through a 3-kDa MW cutoff membrane, and the retentate was purified by Superdex 200 gel filtration column chromatography with 1 × PBS (pH 7.4) as the buffer.

2.8. ELISA

Wells of a 96-well plate (Corning) were coated with trastuzumab Fc variants (4 μg/mL; AglycoT, GlycoT, and AglycoT-HW86) diluted in 0.05 M Na_2CO_3 (pH 9.6) via overnight incubation at 4°C. After blocking with 1 × PBS containing 4% skim milk and incubation at room temperature for 1 h, 4-fold serially diluted monomeric FcγRI, dimeric forms of GST-fused Fc receptors (FcγRIIa-131H-GST, FcγRIIa-131R-GST, FcγRIIb-GST, FcγRIIIa-158V-GST, FcγRIIIa-158F-GST, and FcRn-GST) prepared as described previously (Jo et al., 2018b), and C1q were added (initial concentration: 4 μg/mL for FcγRI; 20 μg/mL for FcγRIIa-131H-GST, FcγRIIa-131R-GST, FcγRIIb-GST, FcγRIIIa-158V-GST, FcγRIIIa-158F-GST, and FcRn-GST; and 100 μg/mL for C1q). After four washes with 1 × PBS containing 0.05% Tween 20, the plate was incubated for 1 h with 1:20,000 diluted mouse anti-His-HRP to detect FcγRI-His; 1:5000 diluted goat anti-GST-HRP to detect FcγRIIa-131H-GST, FcγRIIa-131R-GST, FcγRIIb-GST, FcγRIIIa-158V-GST, FcγRIIIa-158F-GST, and FcRn-GST; and 1:400 diluted anti-C1q-HRP to detect C1q. After four washes with 1 × PBS containing 0.05% Tween 20 and addition of 50 μL of Ultra-TMB substrate (Thermo Fisher Scientific), signal was quenched by adding 2 M sulfuric acid, and absorbance was measured at 450 nm using an Epoch 96 well plate reader (Biotek, Winooski, VT).

2.9. Biolayer interferometry (BLI) analysis

To determine the affinity constant of IgG antibodies, the BLI assay was performed using a BLitz instrument (Pall Fortebio). After activation of the AR2G biosensor via incubation in 20 mM 1-ethyl-3-(3-dimethylaminopropyl)carbodiimide and 10 mM sulfo-*N*-hydroxysuccinimide dissolved in deionized water for 5 min, the biosensor was incubated in 20 μg/mL clinical-grade Herceptin (Roche), GlycoT, and AglycoT-HW86 in 10 mM sodium acetate (pH 5.0) for 5 min for immobilization, and the amine coupling reaction was quenched by incubating the biosensor in 1 M ethanolamine (pH 8.5) for 5 min. Subsequently, the biosensor was equilibrated with 1× kinetics buffer (Pall Fortebio) and associated with 4 μL of monomeric FcγRIIIa-158 V, which was 2-fold serially diluted in 1× kinetics buffer, for 1 min. To dissociate bound FcγRIIIa-158 V, 1× kinetics buffer was added followed by a 1 min incubation. Then, the biosensor was regenerated by alternating incubating steps (5 s 10 mM glycine (pH 1.5) and 1× kinetics buffer, respectively) five times. Finally, we determined equilibrium binding constants of Herceptin, GlycoT, and AglycoT-HW86 by plotting the response at steady-state against each analyzed concentration.

2.10. N-glycan analysis using UPLC

Glycan profiling was performed with a Rapi-Fluor labeling kit (Waters, Milford, USA), which includes IgG standards and other labeling materials. All glycan profiling procedures were performed as described in a previous study (Lim et al., 2019). Briefly, 25 μL of IgG standard or GlycoT was mixed with 6 μL of 5% Rapi-Gest SF and water, then the samples were heated for 3 min at 90°C. After cooling for 3 min and mixing with 1.2 μL of GlycoWorks Rapid PNGaseF for deglycosylation, samples were incubated at 50°C for 5 min and cooled down to room temperature for 3 min, followed by the addition of 12 μL of labeling solution to the mixture and a 5 min incubation. The final solution was diluted with 385 μL of acetonitrile solution for enrichment of labeled glycans. Labeled glycans were purified by using hydrophilic interaction liquid chromatography (HILIC) μElution plates that were washed and primed with 200 μL water and 200 μL of 85% acetonitrile, respectively. Samples were loaded and washed with 600 μL of washing solution (1:9:90 = formic acid:DI water:acetonitrile). Bound glycans were eluted three times with 30 μL elution buffer (200 mM ammonium acetate in 5% acetonitrile) and analyzed with a Waters UPLC-FLR system.

2.11. ADCC assay

SKBR-3 cells (target cells) were cultured in McCoy's medium supplemented with 10% FBS and 1× antibiotic-antimycotic (Thermo Fisher Scientific) at 37°C under 5% CO_2 until reaching approximately 70–80% confluence. Cells were then resuspended in assay buffer (RPMI medium, 10% heat inactivated FBS, 30 ng/mL recombinant human IL-2 [Peprotech, Rocky Hill, NJ]), and 50 μL aliquots of cells (1×10^4) were added to each well of a 96-well plate (V-bottom, Corning). Then, 10 μL

Table 2
Fc variants selected as templates for constructing the shuffled Fc variant library.

Variant	Sites of mutation	Target FcγR	Reference
Fc(Xencor2a)	G236A	FcγRIIa	Lazar et al. (2006)
Fc(Xencor3a)	S239D/A330L/I332E	FcγRIIIa	Richards et al. (2008)
Fc(Xencor2b)	S267E/L328F	FcγRIIb	Chu et al. (2008)
Fc(Macrogenics)	L235V/F243L/R292P/Y300L/P396L	FcγRIIIa	Stavenhagen et al. (2007)
Fc5	E382V/M428I	FcγRI	Jung et al. (2010)
Fc5-2a	S298G/T299A/E382V/M428I	FcγRIIa	Jung et al. (2013)
Fc1004	S298G/T299A/E382V/N390D/M428L	FcγRIIa	Jung et al. (2013)
Fc701	Q295R/L328W/P331A/I332Y/E382V/M428L	FcγRI	Jung et al. (2014)
Fc-A/IYG	T299A/K326I/A327Y/L328G	FcγRIIa	Wittrup et al. (2014)
Fc-MG48	V264E/S298G/T299A/K326I/A327Y/L328G/T350A/E382V/N390D/M428L	FcγRIIIa	Jo et al. (2018b)

each of AglycoT-HW86, GlycoT, and AglycoT prepared via 5-fold serial dilution in assay buffer was added followed by a 1 h incubation at 37°C under 5% CO_2. PBMCs collected and pooled from five anonymous donors (Immunospot, Cleveland, OH) (Supplementary Table S2) were quickly thawed at 37°C, transferred to a 50 mL tube, and mixed with 10 mL of anti-aggregation buffer prepared by mixing 1 mL of CTL Anti-aggregate Wash™ 20× Solution (Immunospot) and 19 mL of RPMI. After mixing once by inversion and centrifugation at 300 × *g* for 10 min, pellets were resuspended in 10 mL of anti-aggregation buffer and centrifuged again at 300 × *g* for 10 min to remove the supernatant. After resuspension in 1 mL of assay buffer and the addition of 50 μL of PBMCs at 2.5 × 10^6/mL to individual wells containing target cells and serially diluted trastuzumab antibodies (AglycoT, GlycoT, and AglycoT-HW86), the 96-well plate was incubated at 37°C for 4 h. The maximum target cell death well was prepared by treating target cells with 10 μL of 0.9% Triton X-100 in PBS; no antibodies or PBMCs were added to this well. Similarly, the well to assess spontaneous effector cell death included only PBMCs without target cells. The plate was centrifuged at 300 × *g* for 5 min, and 50 μL of supernatant from each well was transferred to a SpectraPlate 96-well plate (PerkinElmer, Waltham, MA) and incubated at 25°C for 30 min. After the addition of 50 μL of CytoTox96® Reagent, the reaction was quenched by adding 50 μL stop solution (CytoTox96® Non-Radioactive Cytotoxicity assay kit), and signal was quantified by measuring absorption at 450 nm using a VersaMax plate reader (Molecular Devices, Sunnyvale, CA). ADCC activity was analyzed using the following formula: ADCC cytotoxicity (%) = 100 x (Experimental cell death − Spontaneous target cell death − Spontaneous effector cell death)/(Maximum target cell death − Spontaneous target cell death). The assay was performed in duplicate.

2.12. In silico prediction of potential major histocompatibility complex (MHC) class II epitopes for AglycoT-HW86

A consensus prediction was used to analyze binding of AglycoT-HW86 and GlycoT to HLA-DRB1*0401, an MHC II allele that covers nearly 95% of humans worldwide, using the Immune Epitope Database (Cantor et al., 2011; Wang et al., 2008). Specifically, the 227 amino acid Fc fragment was fragmented into 15-amino acid peptides that were antigenic for MHC II, and the interaction between the antigenic peptides and MHC II was scored as the consensus percentile rank (CPR), with a lower CPR indicating greater binding affinity for MHC II. MHC II binding affinity to core peptides consisting of nine amino acids, which were derived from the 15-amino acid peptides, were analyzed and IC_{50} values of < 50, < 500, and < 5000 nM represented high, intermediate, and low affinity binding, respectively.

3. Results

3.1. Design and construction of an Fc variant shuffled library

Fc engineering studies conducted to improve FcγR binding profiles have reported a number of beneficial mutations for glycosylated or aglycosylated Fc (Park et al., 2016). Combinations of mutations that enhance FcγR binding identified in prior research can be used to generate aglycosylated Fc variants that exhibit better FcγRIIIa binding and ADCC effector function. Additionally, investigating the effect of Fc mutations that enhance the FcγR binding of glycosylated antibodies on the FcγR binding of aglycosylated Fc can provide crucial information about the structure-function relationship of the Fc region. Therefore, we constructed a shuffled Fc variant library using both glycosylated and aglycosylated Fc variants with enhanced FcγR binding because mutations that increase the interaction between FcγRIIIa and glycosylated Fc can affect the binding affinity of aglycosylated Fc for FcγRIIIa. As templates for constructing the shuffled Fc variant library, we used various Fc variants with enhanced binding affinity for FcγRI, FcγRIIa, and FcγRIIb as well as FcγRIIIa because all human FcγRs (FcγRI, FcγRIIa, and FcγRIIb) share the same Fc binding epitope, which is located in the lower hinge region and upper CH2 region (Caaveiro et al., 2015) (Table 2, Supplementary Fig. S1).

For random combinations of previously isolated beneficial mutations, we used equimolar mixtures of oligonucleotides encoding amino acids for wild-type Fc and previously isolated Fc variants at the desired mutation points. Three in-frame partial Fc gene fragments obtained from overlapping PCR and β-lactamase gene selection (Ju et al., 2017) to remove partial genes containing either out-of-frame sequences or stop codons were assembled by PCR, and then the in-frame selected full-length Fc variant genes were obtained using the same β-lactamase selection procedure. For efficient display and high-throughput screening of homodimeric Fc variants, full-length Fc variant genes were subcloned into a plasmid for membrane protein drift and assembly system (MPDA), which allows monomeric Fc polypeptides anchored on bacterial inner membrane via C-terminal gpIII fusion to dimerize and be displayed efficiently (Jo et al., 2018a). The library size of the resulting Fc shuffled library was sufficient (library size: 4.3 × 10^8) to ensure theoretical maximum diversity (2.84 × 10^8), and the sequencing results indicated that the resulting shuffled Fc variant library contained combinations of mutations at the desired amino acid residues (Fig. 1B).

3.2. Identification of optimal combinations of mutations for binding of aglycosylated Fc to FcγRIIIa

To isolate aglycosylated Fc variants with the optimal combinations of mutations for enhanced FcγRIIIa binding affinity, we performed flow cytometric screening using the constructed shuffled aglycosylated Fc library and tetrameric FcγRIIIa-streptavidin-Alexa 488 as a probe (Jo et al., 2018b). After 5 rounds of sorting, spheroplasts displaying Fc variants with high FcγRIIIa binding were enriched, and we isolated an

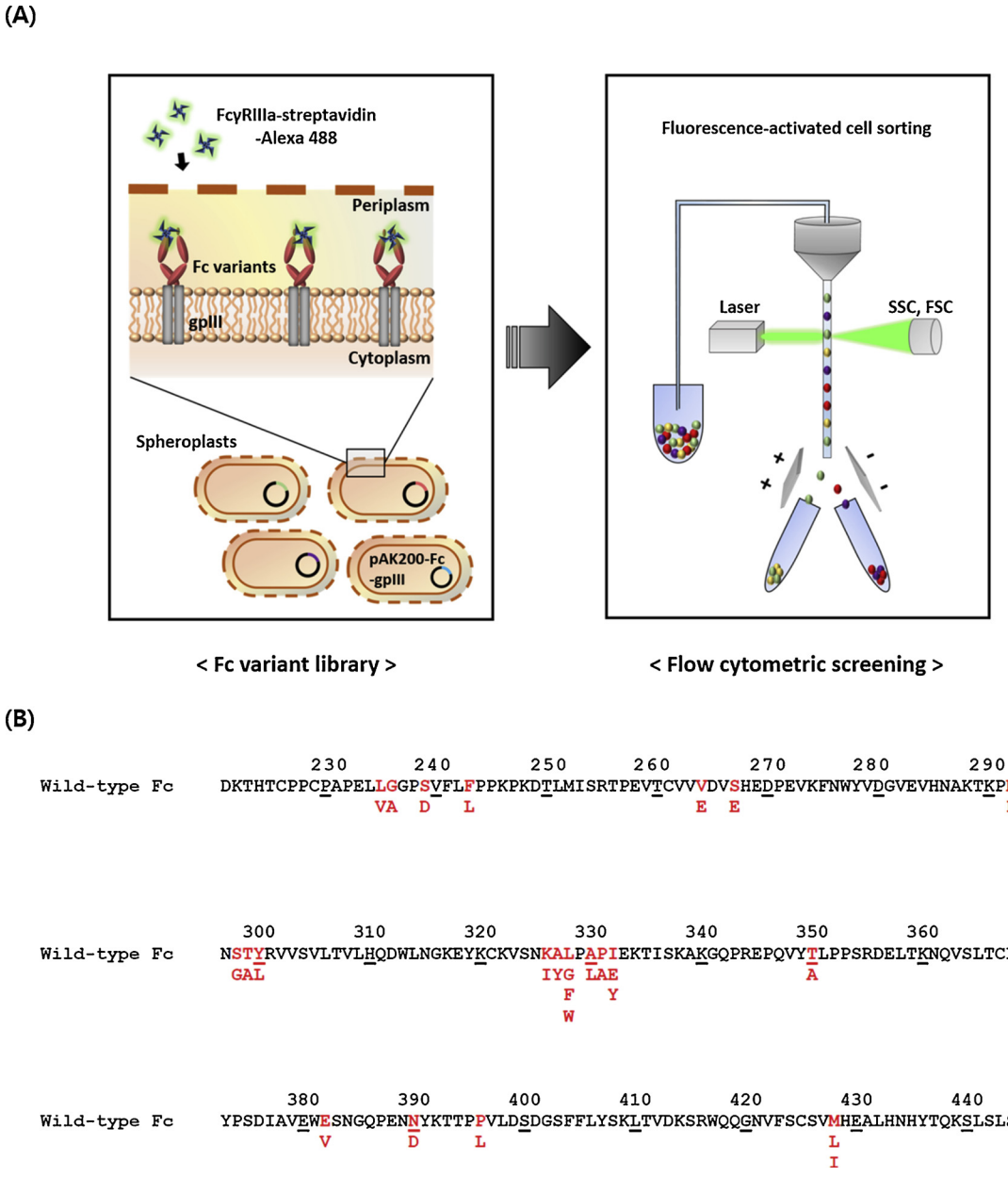

Fig. 1. (A) A schematic diagram representing high-throughput screening of the shuffled Fc variant library. (B) Designed sequences in the shuffled Fc variant library.

Fc variant (Fc-HW86) that exhibited the highest FcγRIIIa binding signal (Fig. 2A). The sequencing results indicated that Fc-HW86 contained the T394A mutation in addition to the mutations featured in Fc-MG48 identified in our previous study (Jo et al., 2018b) (Fig. 2B). Surprisingly, no reported beneficial mutations for glycosylated Fc were selected in the directed evolution process. Because the T394A mutation was not included in any template that was used to construct the shuffled Fc variant library, the mutation was likely introduced during Fc gene recovery through PCR amplification after each round of flow cytometric screening.

Fc-HW86 containing one additional mutation (T394A) displayed a larger FcγRIIIa binding signal than Fc-MG48. To examine the effect of T394A on the binding affinity of other aglycosylated Fc variants for FcγRIIIa, we introduced the mutation into wild-type aglycosylated Fc and Fc1004/IYG (Jo et al., 2018b), and analyzed FcγRIIIa binding signals via fluorescence-activated cell sorting. The result revealed that the T394A mutation also increased the affinities of wild-type aglycosylated Fc and Fc1004/IYG for FcγRIIIa (Fig. 3).

3.3. Affinities of AglycoT-HW86 for Fc binding ligands

Because Fc-HW86 contained a mutation (T299A) in the canonical *N*-linked glycosylation motif (Asn-X-Ser/Thr), resulting in no glycosylation at N297 of Fc, we produced AglycoT-HW86 and GlycoT in HEK293 F cells via transient transfection as reported previously, respectively (Jo et al., 2018b; Jung et al., 2010). AglycoT was produced in *E. coli* MG1655 cells via fed-batch fermentation (Lee et al., 2014).

After purification of AglycoT-HW86, AglycoT, and GlycoT using protein A affinity chromatography followed by gel filtration chromatography (Fig. 4A), binding affinities for both allotype forms of FcγRIIIa, namely FcγRIIIa-158 V and FcγRIIIa-158 F, were analyzed using ELISA. As expected, AglycoT-HW86 exhibited significantly greater binding to both FcγRIIIa-158 V and FcγRIIIa-158 F than GlycoT (Fig. 4 B and C). The quantitative affinities of the trastuzumab Fc variants for FcγRIIIa were measured using a BLI instrument. Although AglycoT-HW86 did not display *N*-linked glycosylation, it exhibited higher affinity with a few-fold lower equilibrium binding constant than GlycoT and clinical-grade Herceptin (Fig. 4 D–F).

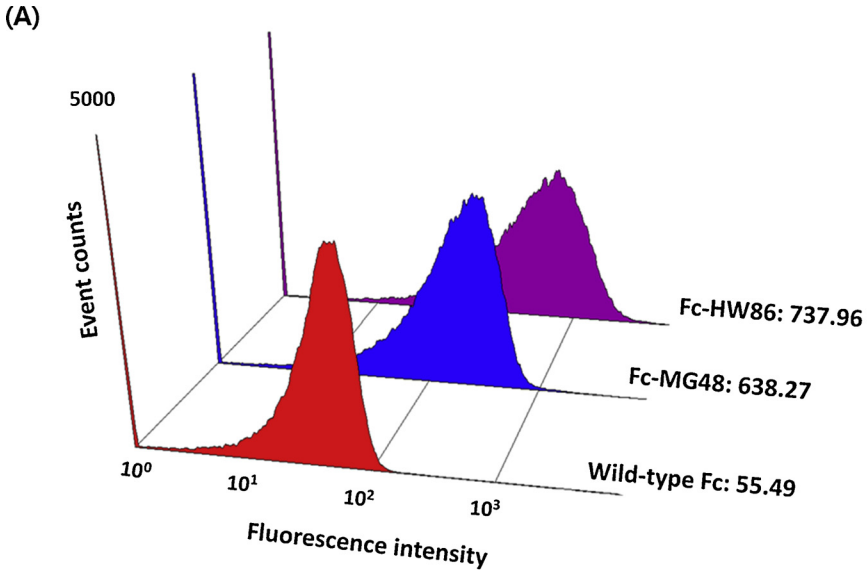

(B)

```
                    230       240       250       260       270       280       290
Wild-type Fc  DKTHTCPPCPAPELLGGPSVFLFPPKPKDTLMISRTPEVTCVVVDVSHEDPEVKFNWYVDGVEVHNAKTKPREEQY
Fc-HW86       ------------------------------------------E-------------------------------

                   300       310       320       330       340       350       360       370
Wild-type Fc  NSTYRVVSVLTVLHQDWLNGKEYKCKVSNKALPAPIEKTISKAKGQPREPQVYTLPPSRDELTKNQVSLTCLVKGF
Fc-HW86       -GA-------------------------IYG--------------------A----------------------

                         380       390       400       410       420       430       440
Wild-type Fc  YPSDIAVEWESNGQPENNYKTTPPVLDSDGSFFLYSKLTVDKSRWQQGNVFSCSVMHEALHNHYTQKSLSLSPGK
Fc-HW86       ---------V-------D---A-------------------------------L-------------------
```

Fig. 2. (A) Fluorescence-activated cell sorting histogram showing the fluorescence intensity of spheroplasts displaying wild-type Fc (red), Fc-MG48 (blue), and Fc-HW86 (purple) upon binding to tetrameric FcγRIIIa-streptavidin-Alexa 488. (B) The sequence of Fc-HW 86 aligned with that of wild-type Fc. (For interpretation of the references to colour in this figure legend, the reader is referred to the web version of this article.)

Binding of the aglycosylated Fc variant to other FcγRs sharing a binding epitope with FcγRIIIa was analyzed via ELISA. Compared to GlycoT, AglycoT-HW86 displayed almost identical binding to FcγRIIa-131H and FcγRIIa-131R, which are predominantly expressed on macrophages and are critical for ADCP effector function (Fig. 5 B and C). Conversely, AglycoT-HW86 had lower FcγRI binding and higher FcγRIIb binding than GlycoT (Fig. 5 A–D). To predict the effect of AglycoT-HW86 mutations on *in vivo* circulating half-life, we measured pH-dependent FcRn binding, which is crucial for intracellular trafficking and recycling of serum IgG antibodies. AglycoT-HW86 had almost identical FcRn binding as GlycoT at a slightly acidic pH (pH 5.8) and efficient dissociation at neutral pH (pH 7.4), suggesting that it may have excellent FcRn binding-mediated recycling and serum persistence. AglycoT-HW86 exhibited slightly lower binding affinity to C1q, which initiates the serum complement-dependent cytotoxicity cascade, than GlycoT (Fig. 5E-G).

3.4. Glycan profiling

Glycan profiling results for the three different antibodies are shown in Supplementary Fig. S2. IgG standard had a very similar glycan pattern to that reported previously (Lim et al., 2019). AglycoT-MG48, the parent antibody of AglycoT-HW86 antibodies, did not produce any glycans as expected because of amino acid substitution of the *N*-glycosylation site (data not shown). Glycans were detected in GlycoT and results were similar to those obtained for the IgG standard. The inset table shows the percentage of each glycan; the extent of glycans with fucose in the IgG standard and GlycoT were 98.62% and 92.56%, respectively. Thus, GlycoT had more fucose free glycans than the IgG standard (Supplementary Fig. S1).

3.5. ADCC analysis and in silico immunogenicity prediction of AglycoT-HW86

To analyze the therapeutic effector function of AglycoT-HW86, we conducted ADCC assays using human PBMCs provided by anonymous donors (Supplementary Table S2) as effector cells and SKBR-3 cells as target cancer cells. As expected, AglycoT, which has no significant binding affinity for any human FcγR, exhibited negligible ADCC activity. In sharp contrast, the ADCC activity of AglycoT-HW86 was over two-fold higher than that of GlycoT (EC_{50} of AglycoT-HW86: 6.0 nM, EC_{50} of GlycoT: 12.7 nM) (Fig. 5H).

Although concerns regarding the immunogenicity of aglycosylated antibodies have been largely dismissed by clinical trials of several aglycosylated antibodies (Ju and Jung, 2014), AglycoT-HW86 contains multiple new mutations in the Fc region. To examine the potential immunogenicity of AglycoT-HW86, we used the Immuno Epitope Database, and the Fc region sequences of AglycoT-HW86 were *in silico*

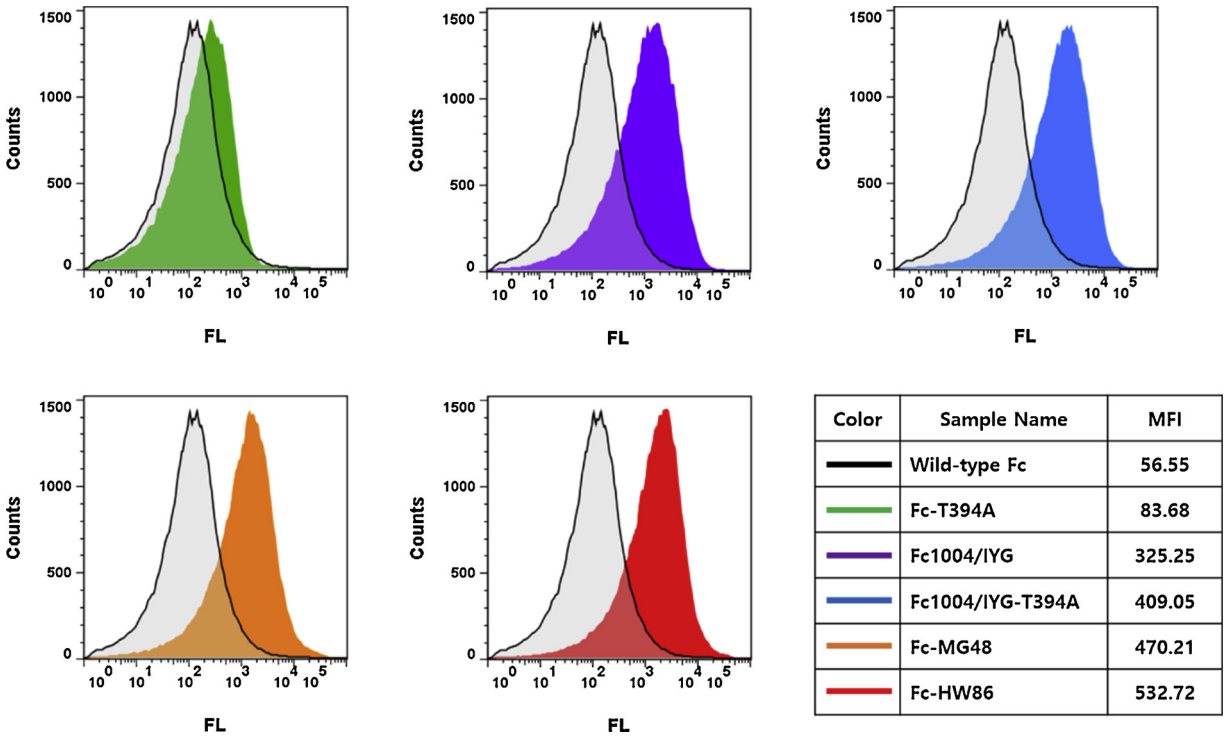

Fig. 3. FACS analysis showing the effect of the T394A substitution on the Fc variants. Spheroplasts displaying Fc variants were labeled with tetrameric FcγRIIIa-streptavidin-Alexa 488, and their fluorescence intensity was analyzed via fluorescence-activated cell sorting.

digested into 9-mer peptides. Next, the binding of the peptides to MHC II allele HLA-DRB1*0401 was predicted, and the CPR was scored. The analysis indicated that AglycoT-HW86 did not have a significantly different CPR score, suggesting that the potential risk of T cell activation and immunogenicity is low (Supplementary Table S3).

4. Discussion

Because binding of IgG antibody to FcγRIIIa directly activates an effector cell's ADCC function, one of the major tumor cell-killing mechanisms for anti-cancer therapeutic antibodies, numerous pharmaceutical companies have been engineering Fc regions for enhanced

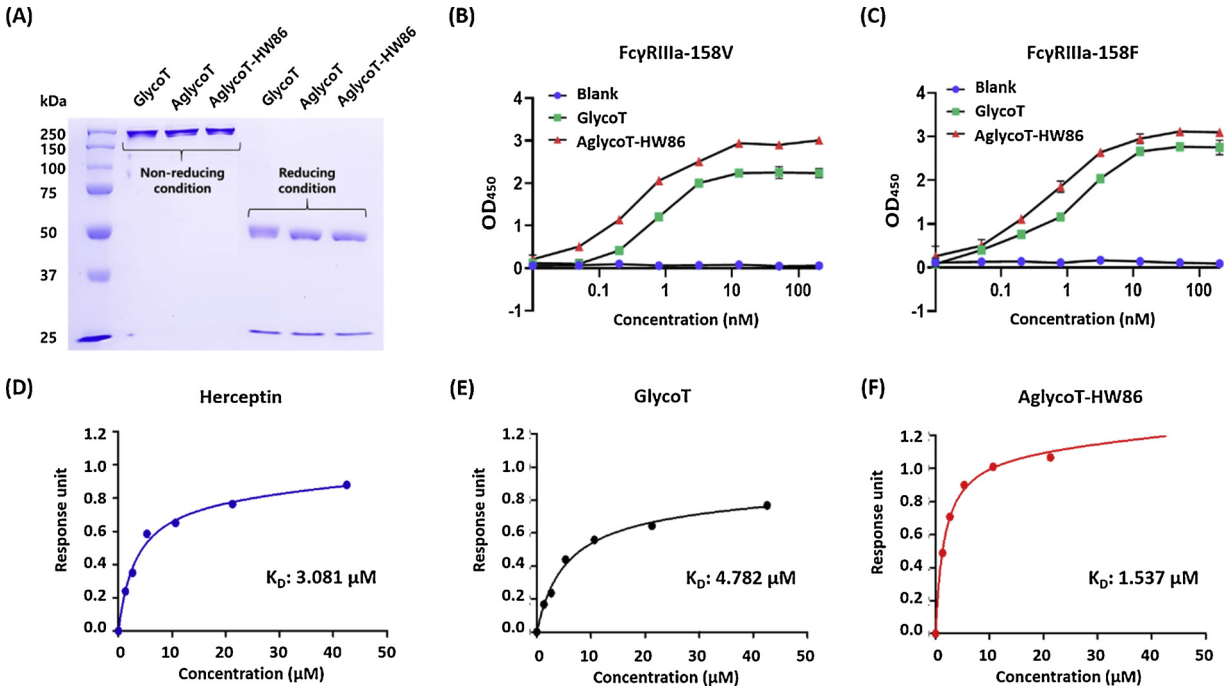

Fig. 4. FcγRIIIa binding affinities of glycosylated trastuzumab (GlycoT), aglycosylated trastuzumab (AglycoT), and aglycosylated trastuzumab-HW86 (AglycoT-HW86). (A) SDS-PAGE showing the trastuzumab Fc variants purified from HEK293 F cells (GlycoT and AglycoT-HW86) and *E. coli* MG1655 cells (AglycoT). (B–C) ELISA results for the binding of trastuzumab Fc variants to FcγRIIIa-158V (B) and FcγRIIIa-158F (C). ELISA assays were performed in duplicate. (D–F) Biolayer interferometry of the equilibrium dissociation constants of clinical-grade Herceptin (D), GlycoT (E), and AglycoT-HW86 (F) for binding to FcγRIIIa-158 V.

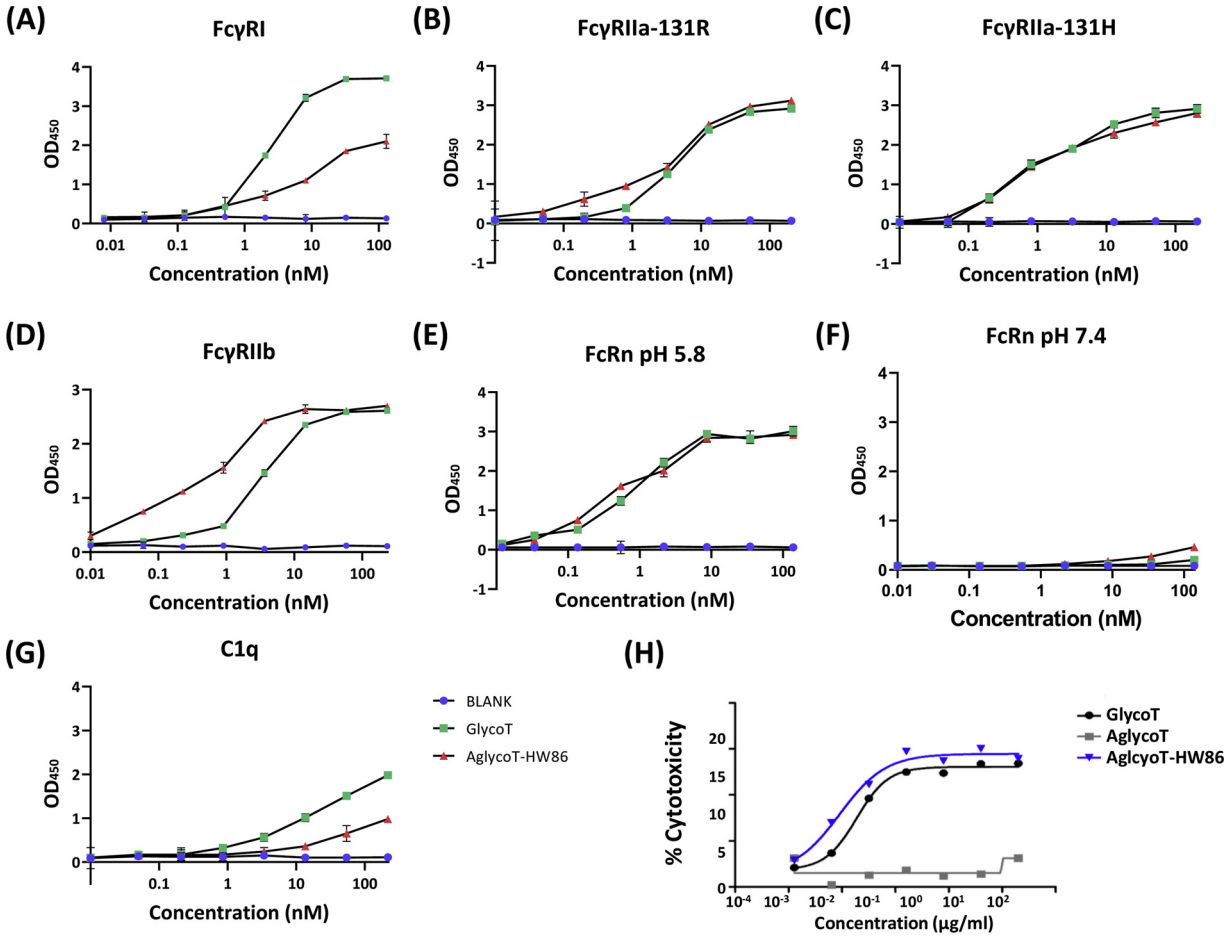

Fig. 5. Analysis of Fc ligand binding profiles and the antibody-dependent cell-mediated cytotoxicity (ADCC) of the Fc variants. (A–G) ELISA of the binding of trastuzumab Fc variants to human FcγRI (A), dimeric human FcγRIIa-131R (B), dimeric human FcγRIIa-131H (C), dimeric human FcγRIIb (D), dimeric human FcRn at pH 5.8 (E), dimeric human FcRn at pH 7.4 (F), and human C1q (G). (H) ADCC of AglycoT (gray), GlycoT (black), and AglycoT-HW86 (blue). (For interpretation of the references to colour in this figure legend, the reader is referred to the web version of this article.)

FcγRIIIa binding (Park et al., 2016). Xencor and Macrogenics have engineered a glycosylated form of Fc that is applicable for conventional mammalian cell culture processes and identified Fc variants that exhibit enhanced FcγR binding affinity (Lazar et al., 2006). Moreover, to overcome the limitations of conventional mammalian cell culture in bioprocessing, such as glycan heterogeneity and high capital investment, as well as enable production in bacteria, various aglycosylated Fc variants have been successfully isolated (Park et al., 2016).

In this study, to identify the best combinations of beneficial mutations for enhanced FcγRIIIa binding by aglycosylated Fc variants, we constructed a shuffled Fc variant library by combining glycosylated and aglycosylated Fc variants identified in previous studies. High-throughput screening of the shuffled Fc variant library using the MPDA display system and flow cytometric screening (Jo et al., 2018a) allowed the enrichment of an aglycosylated Fc variant that exhibited approximately three-fold higher FcγRIIIa binding and over two-fold enhanced ADCC activity.

Interestingly, most mutations that enhanced the FcγRIIIa binding affinity of glycosylated Fc variants were not observed in aglycosylated Fc variants with enriched FcγRIIIa binding. In addition, the best FcγRIIIa-binding aglycosylated Fc variant (Fc-HW86) did not contain any beneficial mutation from previously engineered glycosylated Fc variants. The *N*-linked glycan at Asn297 of IgG1 bulges out both chains of Fc, and its presence significantly alters the conformation of the upper CH2 region (Borrok et al., 2012; Lee and Im, 2017; Subedi and Barb, 2015). Based on single-molecule FRET analysis (Ju et al., 2015) and small angle X-ray scattering results (Borrok et al., 2012), aglycosylated Fc variants have an upper CH2 region with a significantly different conformation and flexibility compared to that of glycosylated counterparts, which is critical for FcγRIIIa binding affinity and subsequent therapeutic effector functions. In good agreement with the structural interpretations, the distribution of previously isolated beneficial mutations for aglycosylated Fc variants differed significantly from those of engineered glycosylated Fc variants. Mutations that enhanced the FcγR binding of aglycosylated Fc variants were mostly distributed over the entire Fc region, ranging from mutations located at the putative FcγR binding site to mutations distant from the FcγR binding epitope (Jo et al., 2018b; Jung et al., 2014, Jung et al., 2013; Jung et al., 2010; Sazinsky et al., 2008). In sharp contrast, most mutations that enhanced the FcγRIIIa binding of glycosylated Fc variants are localized in the lower hinge and upper CH2 regions, which are putative Fc binding epitopes (Chu et al., 2008; Lazar et al., 2006; Richards et al., 2008; Stavenhagen et al., 2007).

In this study, we identified the T384A mutation, which improved the FcγRIIIa binding affinity of aglycosylated Fc variants. AglycoT-HW86, which contained this mutation together with several previous mutations exhibited greater FcγRIIIa binding affinity and enhanced cytotoxicity against tumor cells than GlycoT when PBMCs were used as effector cells. AglycoT-HW86 exhibited increased binding affinity to both activating FcγRIIa-131R and inhibitory FcγRIIb in addition to enhanced FcγRIIIa binding. Previous research indicated that the ADCP activity of macrophages was largely affected by selectivity for FcγRIIa over FcγRIIb (Jung et al., 2013), and macrophages also express FcγRIIIa on their surface. How these different affinities of AglycoT-HW86 for

FcγRs affect ADCP activity will be explored in future studies. AglycoT-HW86 mutations did not appear to be problematic based on *in silico* immunogenicity analysis, but more elaborate immunogenicity validations are needed prior to clinical applications.

Taken together, these results strongly indicate that to improve the FcγR binding and effector functions of aglycosylated antibodies, a novel engineering strategy and a set of mutations distinctive from those in glycosylated Fc variants are necessary to stabilize the flexible conformation of aglycosylated Fc. Various engineered aglycosylated Fc variants produced via distinctive engineering approaches from those employed in glycosylated Fc engineering will provide a platform for producing therapeutic aglycosylated antibodies with improved potency, and the resulting FcγR-specific Fc variants are likely to be highly valuable tools for regulating the activity of various immune cells in applied immunology research.

Acknowledgements

This work was supported by grants from the Basic Science Research Program (2019R1F1A1059834), the Bio & Medical Technology Development Program (2017M3A9C8060541), and the Pioneer Research Center Program (2014M3C1A3051460) through the National Research Foundation of Korea funded by the Ministry of Science and ICT.

Appendix A. Supplementary data

Supplementary material related to this article can be found, in the online version, at doi:https://doi.org/10.1016/j.molimm.2019.07.007.

References

Borrok, M.J., Jung, S.T., Kang, T.H., Monzingo, A.F., Georgiou, G., 2012. Revisiting the role of glycosylation in the structure of human IgG Fc. ACS Chem. Biol. 7, 1596–1602.

Caaveiro, J.M.M., Kiyoshi, M., Tsumoto, K., 2015. Structural analysis of Fc/FcγR complexes: a blueprint for antibody design. Immunol. Rev. 268, 201–221.

Cantor, J.R., Yoo, T.H., Dixit, A., Iverson, B.L., Forsthuber, T.G., Georgiou, G., 2011. Therapeutic enzyme deimmunization by combinatorial T-cell epitope removal using neutral drift. Proc. Natl. Acad. Sci. U. S. A. 108, 1272.

Chu, S.Y., Vostiar, I., Karki, S., Moore, G.L., Lazar, G.A., Pong, E., Joyce, P.F., Szymkowski, D.E., Desjarlais, J.R., 2008. Inhibition of B cell receptor-mediated activation of primary human B cells by coengagement of CD19 and FcγRIIb with Fc-engineered antibodies. Mol. Immunol. 45, 3926–3933.

Grilo, A.L., Mantalaris, A., 2019. The increasingly human and profitable monoclonal antibody market. Trends. Biotechnol. 37, 9–16.

Jo, M., Hwang, B., Yoon, H.W., Jung, S.T., 2018a. *Escherichia coli* inner membrane display system for high-throughput screening of dimeric proteins. Biotechnol. Bioeng. 115, 2845–2848.

Jo, M., Kwon, H.S., Lee, K.-H., Lee, J.C., Jung, S.T., 2018b. Engineered aglycosylated full-length IgG Fc variants exhibiting improved FcγRIIIa binding and tumor cell clearance. mAbs 10, 278–289.

Ju, M.S., Jung, S.T., 2014. Aglycosylated full-length IgG antibodies: steps toward next-generation immunotherapeutics. Curr. Opin. Biotechnol. 30, 128–139.

Ju, M.-S., Na, J.-H., Yu, Y.G., Kim, J.-Y., Jeong, C., Jung, S.T., 2015. Structural consequences of aglycosylated IgG Fc variants evolved for FcγRI binding. Mol. Immunol. 67, 350–356.

Ju, M.S., Min, S.W., Lee, S.M., Kwon, H.S., Park, J.C., Lee, J.C., Jung, S.T., 2017. A synthetic library for rapid isolation of humanized single-domain antibodies. Biotechnol. Bioprocess Eng. 22, 239–247.

Jung, S.T., Reddy, S.T., Kang, T.H., Borrok, M.J., Sandlie, I., Tucker, P.W., Georgiou, G., 2010. Aglycosylated IgG variants expressed in bacteria that selectively bind FcγRI potentiate tumor cell killing by monocyte-dendritic cells. Proc. Natl. Acad. Sci. U. S. A. 107, 604.

Jung, S.T., Kelton, W., Kang, T.H., Ng, D.T.W., Andersen, J.T., Sandlie, I., Sarkar, C.A., Georgiou, G., 2013. Effective phagocytosis of low Her2 tumor Cell lines with engineered, aglycosylated IgG displaying high FcγRIIa affinity and selectivity. ACS Chem. Biol. 8, 368–375.

Jung, S.T., Kang, T.H., Kim, D.-i., 2014. Engineering an aglycosylated Fc variant for enhanced FcγRI engagement and pH-dependent human FcRn binding. Biotechnol. Bioprocess Eng. 19, 780–789.

Kawarasaki, Y., Griswold, K.E., Stevenson, J.D., Selzer, T., Benkovic, S.J., Iverson, B.L., Georgiou, G., 2003. Enhanced crossover SCRATCHY: construction and high-throughput screening of a combinatorial library containing multiple non-homologous crossovers. Nucleic Acids Res. 31, e126.

Krebber, A., Bornhauser, S., Burmester, J., Honegger, A., Willuda, J., Bosshard, H.R., Plückthun, A., 1997. Reliable cloning of functional antibody variable domains from hybridomas and spleen cell repertoires employing a reengineered phage display system. J. Immunol. Methods 201, 35–55.

Lazar, G.A., Dang, W., Karki, S., Vafa, O., Peng, J.S., Hyun, L., Chan, C., Chung, H.S., Eivazi, A., Yoder, S.C., Vielmetter, J., Carmichael, D.F., Hayes, R.J., Dahiyat, B.I., 2006. Engineered antibody Fc variants with enhanced effector function. Proc. Natl. Acad. Sci. U. S. A. 103, 4005.

Lee, H.S., Im, W., 2017. Effects of *N*-Glycan composition on structure and dynamics of IgG1 Fc and their implications for antibody engineering. Sci. Rep. UK. 7, 12659.

Lee, Y.J., Lee, D.H., Jeong, K.J., 2014. Enhanced production of human full-length immunoglobulin G1 in the periplasm of *Escherichia coli*. Appl. Microbiol. Biotechnol. 98, 1237–1246.

Lim, M.S., So, M.K., Lim, C.S., Song, D.H., Kim, J.W., Woo, J., Ko, B.J., 2019. Validation of Rapi-Fluor method for glycan profiling and application to commercial antibody drugs. Talanta 198, 105–110.

Nordstrom, J.L., Gorlatov, S., Zhang, W., Yang, Y., Huang, L., Burke, S., Li, H., Ciccarone, V., Zhang, T., Stavenhagen, J., Koenig, S., Stewart, S.J., Moore, P.A., Johnson, S., Bonvini, E., 2011. Anti-tumor activity and toxicokinetics analysis of MGAH22, an anti-HER2 monoclonal antibody with enhanced Fcγ receptor binding properties. Breast Cancer Res. 13, R123.

Park, H.I., Yoon, H.W., Jung, S.T., 2016. The highly evolvable antibody Fc domain. Trends Biotechnol. 34, 895–908.

Reichert, J.M., 2017. Antibodies to watch in 2017. mAbs 9, 167–181.

Richards, J.O., Karki, S., Lazar, G.A., Chen, H., Dang, W., Desjarlais, J.R., 2008. Optimization of antibody binding to FcγRIIa enhances macrophage phagocytosis of tumor cells. Mol. Cancer Ther. 7, 2517–2527.

Sazinsky, S.L., Ott, R.G., Silver, N.W., Tidor, B., Ravetch, J.V., Wittrup, K.D., 2008. Aglycosylated immunoglobulin G1 variants productively engage activating Fc receptors. Proc. Natl. Acad. Sci. U. S. A. 105, 20167–20172.

Stavenhagen, J.B., Gorlatov, S., Tuaillon, N., Rankin, C.T., Li, H., Burke, S., Huang, L., Vijh, S., Johnson, S., Bonvini, E., Koenig, S., 2007. Fc optimization of therapeutic antibodies enhances their ability to kill tumor cells *in vitro* and controls tumor expansion *in vivo* via low-affinity activating Fcgamma receptors. Cancer Res. 67, 8882–8890.

Subedi, Ganesh P., Barb, Adam W., 2015. The structural role of antibody *N*-glycosylation in receptor interactions. Structure 23, 1573–1583.

Walsh, G., 2018. Biopharmaceutical benchmarks 2018. Nat. Biotechnol. 36, 1136.

Wang, P., Sidney, J., Dow, C., Mothé, B., Sette, A., Peters, B., 2008. A systematic assessment of MHC class II peptide binding predictions and evaluation of a consensus approach. PLoS Comput. Biol. 4, e1000048.

Wittrup, K.D., Ravetch, J.V., Sazinsky, S.L., 2014. Aglycosylated Immunoglobulin Mutants. United States Patent 8815237. .